

## Effect of pre-stressed cable on pre-stressed mega-braced steel frame

Tang Baijian<sup>a</sup>, Zhang Fuxing<sup>b</sup>, Wang Yi<sup>c</sup> and Wang Fei<sup>\*</sup>

School of Civil Engineering and Architecture, Jiangsu University of Science and Technology,  
2 Mengxi Road, Zhenjiang 212003, China

(Received May 15, 2015, Revised March 31, 2016, Accepted May 24, 2016)

**Abstract.** This study addresses the effect of pre-stressed cables on a pre-stressed mega-braced steel frame through employing static analysis and pushover analysis. The performances of a pre-stressed mega-braced steel frame and a pure steel frame without mega-braces are compared in terms of base shear, ductility, and failure mode. The influence of the cable parameters is also analyzed. Numerical results show that cable braces can effectively improve the lateral stiffness of a pure frame. However, it reduces structural ductility and degenerates structural pre-failure lateral stiffness greatly. Furthermore, it is found that 20% fluctuation in the cable pretension has little effect on structural ultimate bearing capacity and lateral stiffness. As comparison, 20% fluctuation in the cable diameter has much greater impact.

**Keywords:** steel frame; pre-stressed mega-brace; pushover analysis; lateral stiffness; failure mode

---

### 1. Introduction

Braces are one of the most commonly used structural elements. They are used as a load-carrying system to resist lateral actions such as earthquakes and wind. A braced frame shows high lateral stiffness in the elastic range of deformation. This system undertakes large lateral displacement in the inelastic range of deformations when subjected to strong ground motions. In that case, the inelastic structural behavior of the braced frames is strongly dependent on the behavior of the bracing members. Many studies have investigated bracing strategies (Chou *et al.* 2014, Asgarian and Moradi 2011, Kim *et al.* 2014) as well as the performances of various braced frames in terms of factors such as the bearing capacity, ductility, and energy dissipation (Esmaeili *et al.* 2013, Asghari and Gandomi 2015, Pandikkadavath and Sahoo 2015). Tang and Gu (2010a, b) have developed a pre-stressed mega-braced steel frame system, where pre-stressed cable mega-braces are used as mega-bracing members in a pure steel moment-resisting frame to improve structural lateral stiffness and lateral resistance. This system avoids the need for complex connections in the braced steel frame structure, thus allows a smaller amount of steel and in turn,

---

\*Corresponding author, Ph.D., E-mail: faye@just.edu.cn

<sup>a</sup>Professor, E-mail: tangbaijian@163.com

<sup>b</sup>M.D. Student, E-mail: zhang.fuxing@foxmail.com

<sup>c</sup>M.D. Student, E-mail: wyiw10000@163.com

reduces structural weight.

In this study, a pre-stressed mega-braced steel frame (PMBF) and a conventional pure steel frame (PF) without any braces were compared in terms of the mechanical performances, such as base shear, ductility, and failure mode. Furthermore, the influence of two important cable parameters—pretension and diameter—was analyzed.

## 2. Numerical analysis model

A PMBF with 15 stories and 4 bays was designed in accordance with the requirements of the Chinese Code for Seismic Design of Buildings (GB50011 2010). By only removing the pre-stressed mega-braces in this PMBF, a pure steel frame (PF) was obtained for comparing. Their two-dimensional frame models were built as shown in Fig. 1. Each floor is 3.6 m high, and each span is 6 m wide. In PMBF, an X-type pre-stressed mega-brace is set for every five stories. All members were made of Q345B steel ( $F_y=345$  MPa) with elastic modulus, coefficient of linear expansion, and density of 206 GPa,  $1.2 \times 10^{-5}$ , and  $7850$  kg/m<sup>3</sup>, respectively. The pre-stressed cable has yield strength, elastic modulus, and coefficient of linear expansion of 1670 MPa, 195 GPa, and  $1.32 \times 10^{-5}$ , respectively.

The dead and live loads are  $4.5$  kN·m<sup>-2</sup> and  $2.5$  kN·m<sup>-2</sup>, respectively. The basic wind pressure  $\omega_0$  is  $0.4$  kN/m<sup>2</sup> (left to right), and the value of the wind pressure height variation coefficient is determined by the C class terrain roughness according to the Chinese load code (GB50009 2012). The seismic design intensity is 8 degrees (PGA=0.2 g), and the construction site is classified as Seismic Use Group I and Soil type II (GB50011 2010).

The structural steel member sizes were determined based on the current Chinese steel structure code (GB50017 2003), as listed in Table 1. The cross-sectional areas and prestress loads of the cables (Table 2) can be found in the papers by Gu and Tang (Gu *et al.* 2011, Tang and Gu 2010b).

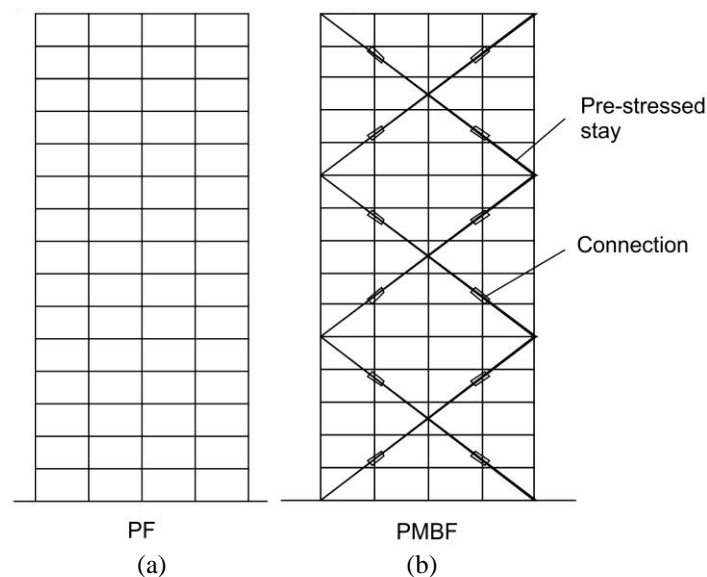


Fig. 1 Typical steel frame model

Table 1 Member sizes of PMBF

Member	Cross section	$H$ (mm)	$B$ (mm)	$T$ (mm)	$T_w$ (mm)
Columns of stories 1–5	H	380	270	16	10
Columns of stories 6–10		310	210	14	9
Columns of stories 11–15		250	170	11	7
Beams		250	125	6	9

Table 2 Diameter and pretension of cable

Location of cable	Diameter (mm)	Cross-sectional area (mm <sup>2</sup> )	Simulated temperature (°C)	Initial pretension (kN)	Initial pre-stress (MPa)
Bottom	18.5	452.16	-90	75.0	60.94
Middle	31	754.39	-44.5	51.5	29.48
Top	18	268.67	-36	20.6	15.17

In these papers, a cooling method was adopted to impose prestress loads with the corresponding negative temperatures listed in Table 2.

The natural period of PMBF is 3.166 s, and 6.950 s for PF.

### 3. Static analysis

The static nonlinear analyses were performed using the software SAP2000. The cable was set as a tension only member. Once the cable is compressed, it will automatically quit from working.

#### 3.1 Dead load+0.5×live load

Static nonlinear analyses of PF and PMBF under the dead load and one-half of the live load ( $D+0.5L$ ) were performed to obtain the stress ratios of these two structures, as shown in Fig. 2.

The stress ratios of the beams in PF are varying from 0.712 to 0.869; for the columns they are varying from 0.288 to 0.619, as shown in Fig. 2(a). In PMBF, the stress ratios of the beams are varying from 0.711 to 0.868; for the columns they are varying from 0.291 to 0.619, as shown in Fig. 2(b). A comparison between Fig. 2(a)-(b) shows that the stress ratios of the two structures are nearly the same, indicating that the mega cable brace has little impact on the mechanical behavior of the structure under vertical loads.

#### 3.2 Dead load+0.5×Live load+Wind load

Static nonlinear analyses of PF and PMBF under the dead load plus one-half of the live load and the wind load ( $D+0.5L+W$ ) were performed. The obtained stress ratio figures and deformation figures are shown in Figs. 3 and 4, respectively.

Fig. 3 shows that in PF around 80% of stress ratios in the frame beams are larger than 1.0 with



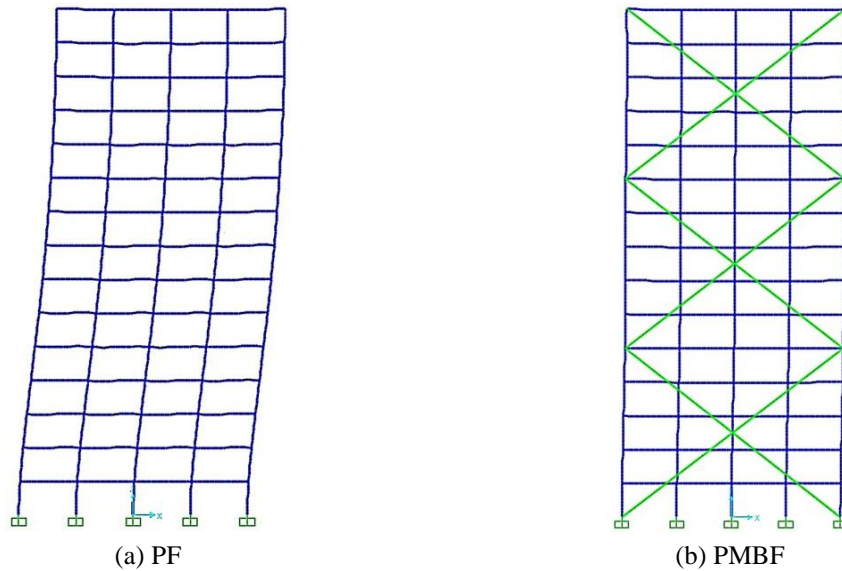
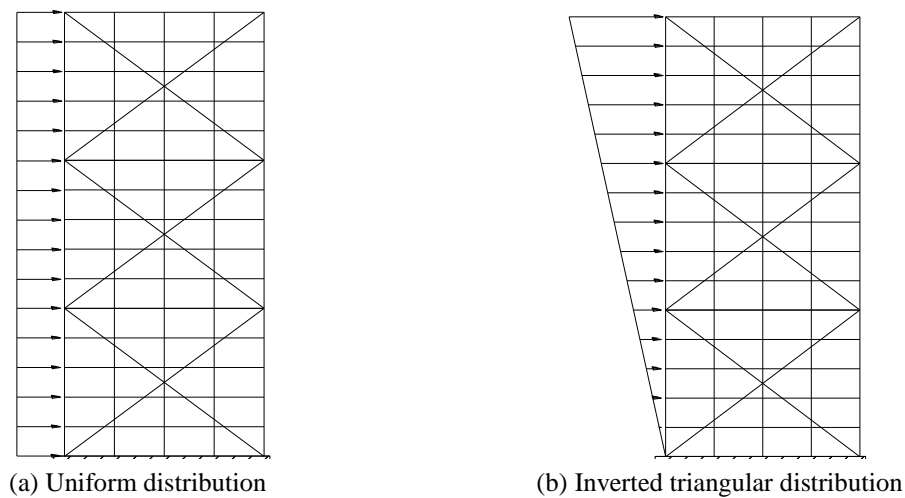
Fig. 4 Deformation of structure under  $D+0.5L+W$ 

Fig. 5 Horizontal load distribution pattern

the maximum and minimum values of 1.632 and 0.734, respectively. The maximum stress ratio of the frame column is 0.956 in PF. The stress ratios of all PMBF members are smaller than 1.0. The stress ratios in the frame beams are 0.8 or so, and the maximum and minimum values are 0.906 and 0.707, respectively. The average stress ratio in the frame columns is about 0.6 and the maximum stress ratio is 0.703. A comparison between PF and PMBF shows that the mega brace of PMBF has a great effect on its bearing capacity when horizontal loads are applied. Fig. 4 shows that the deformation of PMBF is significantly smaller than that of PF under the same loads, indicating that pre-stressed mega-braces can effectively improve structural lateral stiffness and hence reduce the lateral deformation of the frame.

#### 4. Pushover analysis

Because different lateral load distributions over the building height will produce different structural failure modes and bearing capacity values, selecting a reasonable lateral load distribution is the first step for pushover analysis. Typical lateral load distributions include uniform distribution, inverted triangular distribution, exponential distribution, and so on. It is generally considered that uniform and inverted triangular distribution can determine upper and lower bounds of structural bearing capacity (Esmaili *et al.* 2013). In this study, they were both used for pushover analysis (See Fig. 5).

The pushover analyses were performed based on FEMA 356 (2000) by using the software SAP2000 and  $P-\Delta$  effects were considered. PMM hinges were set at two ends of the frame columns;  $M$  and  $V$  hinges, at two ends of the frame beams; and  $P$  hinges, at the middle of the pre-stressed cables. All plastic hinges were of FEMA type (Khandelwal *et al.* 2009).

##### 4.1 Base shear and ductility

After the pushover analyses of PMBF and PF under uniformly distributed horizontal load and inverted triangular horizontal load were performed, the base shear-roof drift curve of the two structures was obtained.

As shown in Fig. 6, the base shear of PMBF is significantly larger than that of PF under the same horizontal loads, indicating that the lateral stiffness of the former is larger than that of the latter. However, the roof drift of PF before it is destroyed is larger than that of PMBF, indicating that the latter has worse ductility than the former.

Ductility is usually expressed in terms of the ductility factor  $\mu$ , which can be measured by the ratio of the ultimate drift  $\Delta_u$  and yield drift  $\Delta_y$ . The larger the ductility factor, the better is the seismic performance of the structure. The ultimate drift  $\Delta_u$  is the corresponding roof drift for the load dropping to 85% of the maximum load. The yield drift  $\Delta_y$  can be determined by the energy equivalence or geometric drawing method. In this study, the geometric drawing method is applied to determine the structural yield and ultimate drifts as shown in Fig. 7.

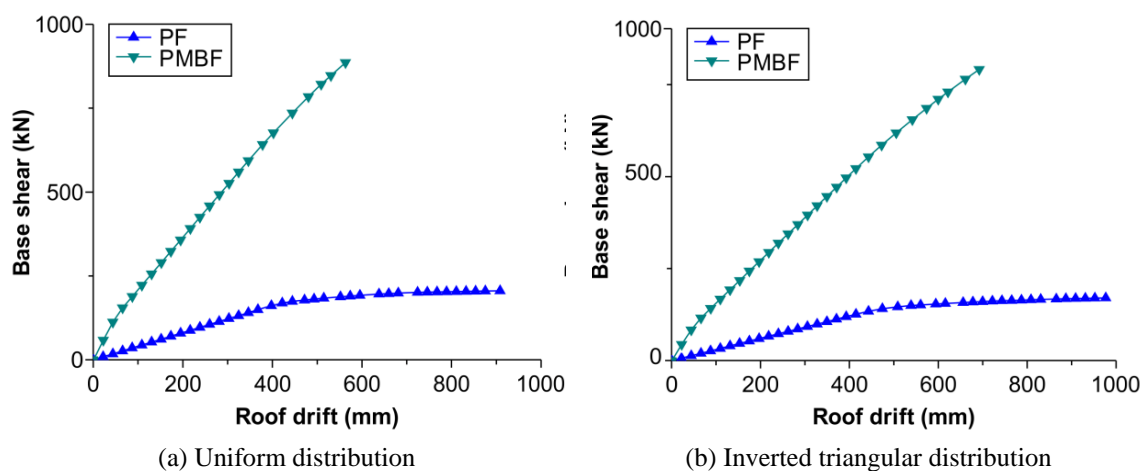


Fig. 6 Base shear-roof drift curve

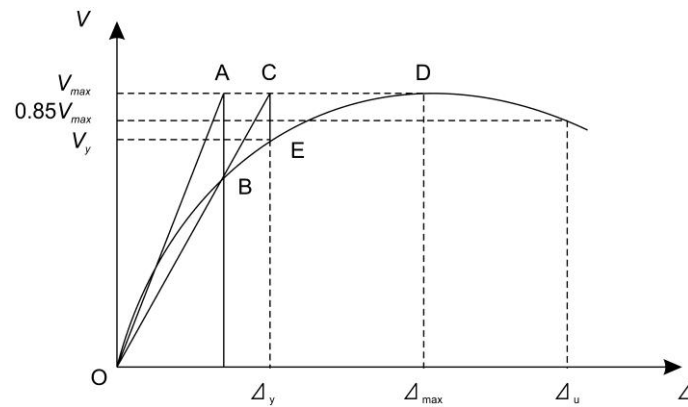


Fig. 7 Determination of yield drift

Table 3 Yield drift, ultimate drift, and ductility factor of structures

Horizontal load mode	Structure type	$\Delta_y$ (mm)	$\Delta_u$ (mm)	$\mu$
Uniform distribution	PMBF	516.56	563.16	1.09
	PF	579.10	908.53	1.57
Inverted triangular distribution	PMBF	621.38	686.06	1.10
	PF	638.03	968.20	1.52

As shown in Table 3, the ductility factor of PMBF from the uniform pushover analysis is 1.09 with a drop of 30.57% compared to that of PF. The ductility factor of PMBF from the triangular pushover analysis is 1.1, while this value for PF is 1.52. So the drop is 27.63%. It shows that the ductility of the frame decreases obviously for the existence of the pre-stressed mega-braces. Meanwhile, the ductility factors are very close in uniform pushover analysis and in triangular pushover analysis for both PMBF and PF, but their ultimate displacements in triangular pushover analysis are 10%-20% larger than those in uniform pushover analysis.

## 4.2 Lateral stiffness and stiffness degradation factor

### 4.2.1 Lateral stiffness

Based on the base shear-roof drift curve, the lateral stiffness-roof drift curve can be obtained. From Fig. 8, the lateral stiffness of PMBF is more than 4 times that of PF, which indicates that the mega-brace can effectively improve the lateral stiffness of the frame. Cables presents two kinds of stress state, which are the stress-increased state and stress-decreased state respectively, when a PMBF is subjected to horizontal external loads. Due to the existence of prestressing, the stress-decreased cable of the X-type brace can provide lateral stiffness as well as the stress-increased one during early stages. However, with the monotonic increase of horizontal loads, the tensile force in the stress-decreased cable is decreasing till to zero when the stress-decreased cable ceases to working. Therefore, as shown in Fig. 8, the lateral stiffness of the structure decreases continuously until all the compression-side cables are disabled. After that, the lateral stiffness of the structure enters a relatively stable stage until the structure reaches the ultimate state. However, the lateral stiffness of PF is relatively flat.

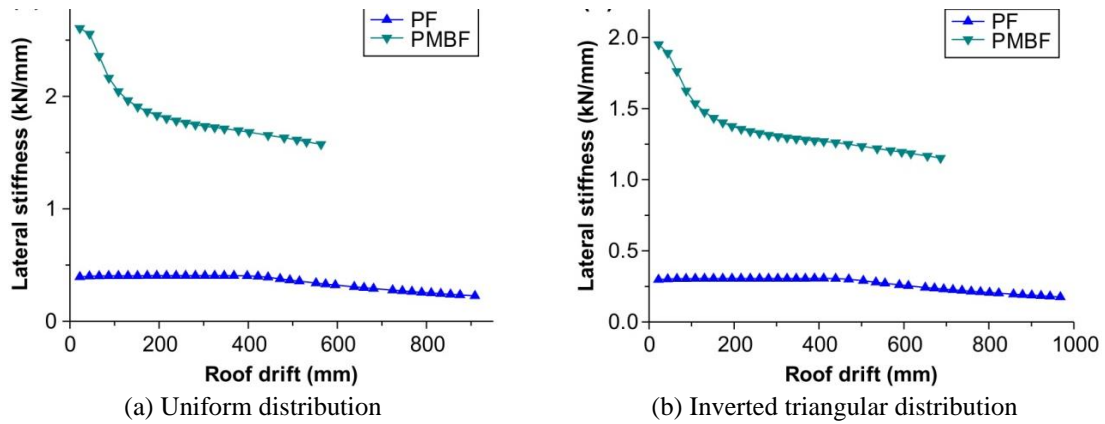


Fig. 8 Lateral stiffness-roof drift curve

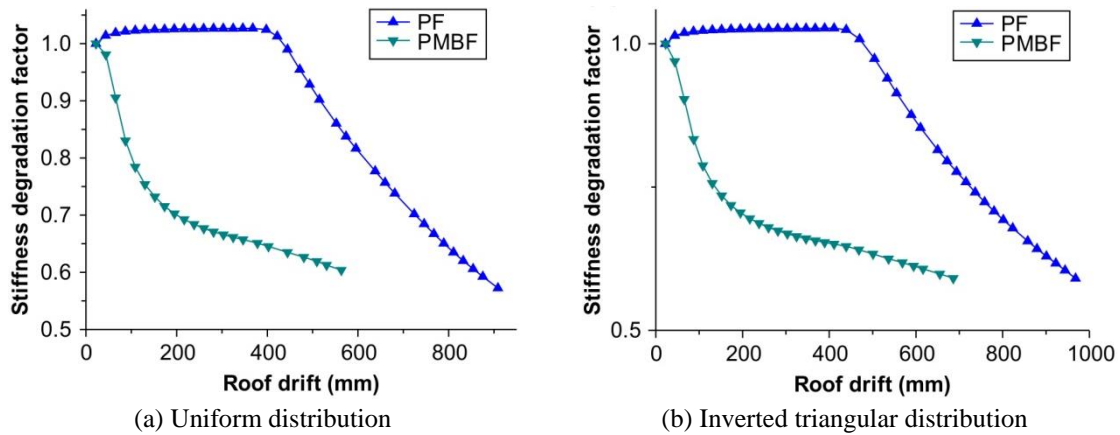


Fig. 9 Stiffness degradation factor-roof drift curve

#### 4.2.2 Stiffness degradation factor

The stiffness degradation factor is the ratio of the instantaneous structural lateral stiffness ( $K_1$ ) in the horizontally loading process to the structural initial lateral stiffness ( $K_0$ ). It can be used to reflect the degradation rate of the lateral stiffness of the structure. The lateral stiffness obtained in the first load step during the pushover analysis is taken as  $K_0$ , and that at other load steps is taken as  $K_1$ . Then, the corresponding stiffness degradation factors can be determined with the stiffness degradation factor-roof drift curve as shown in Fig. 9.

Fig. 9 shows that the lateral stiffness of PF mainly remains unchanged during early stages and then decreases almost linearly with the increasing roof drift after a certain point. However, for PMBF, the lateral stiffness firstly decreases linearly, and then becomes flat after some stress-decreased cables stop working.

#### 4.3 Structural failure mode

##### 4.3.1 Uniform distribution

Plastic hinges begin to appear in the frame beams for PF at the load of 160.94 kN with the

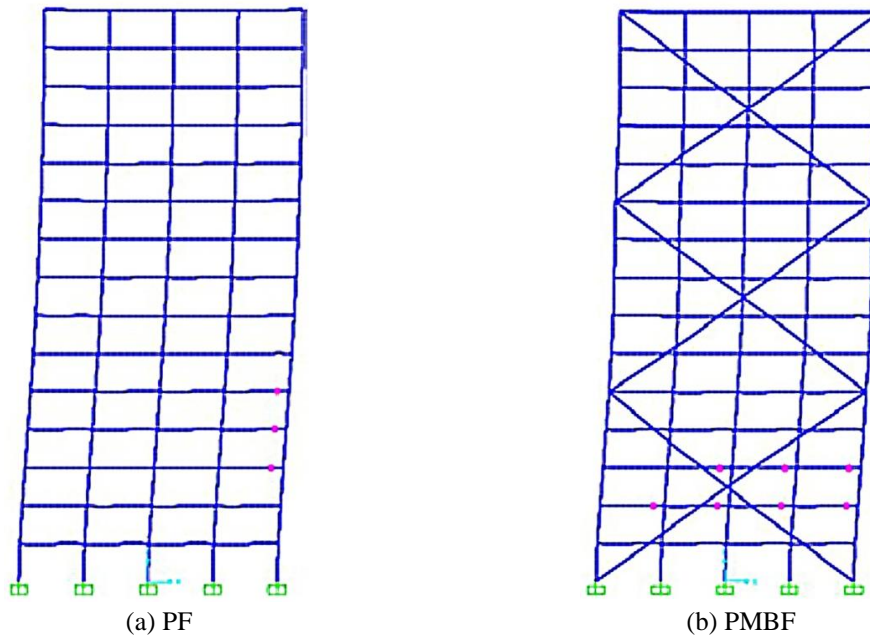


Fig. 10 Plastic hinge distribution when it begins to appear in beam under uniformly horizontal load

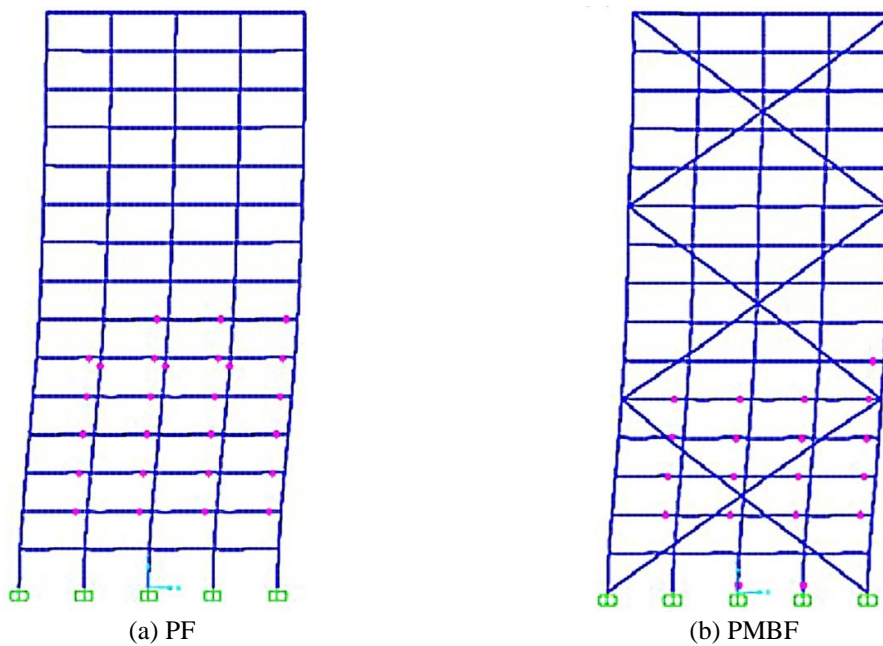


Fig. 11 Plastic hinge distribution when they begins to appear in column under uniformly horizontal loads

corresponding roof drift of 397.71 mm. For PMBF, plastic hinges begin to appear in the beams of the bottom mega-frame at the load is 641.59 kN with the roof drift of 378.25 mm, as shown in Fig. 10.

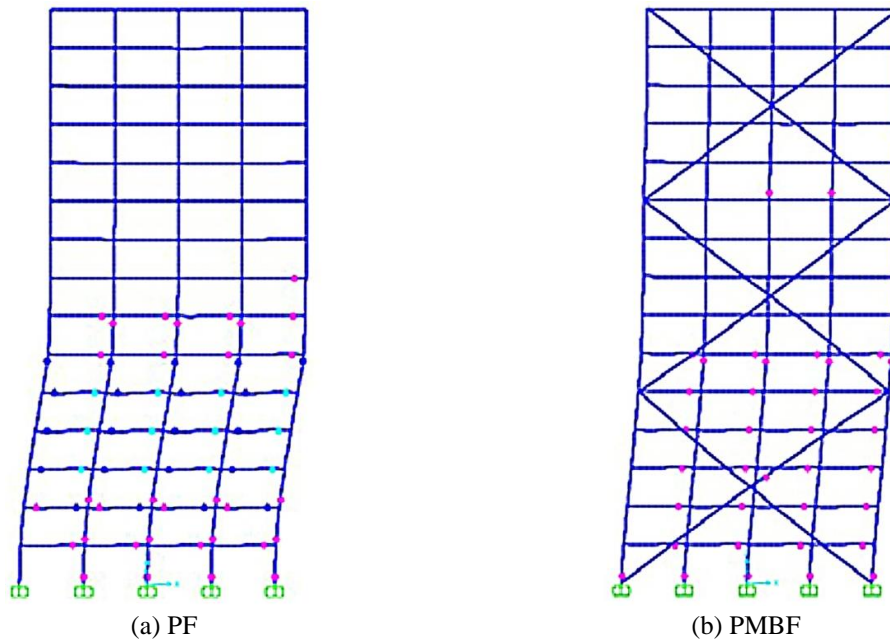


Fig. 12 Plastic hinge distribution when the ultimate bearing capacity state is reached under uniformly horizontal load

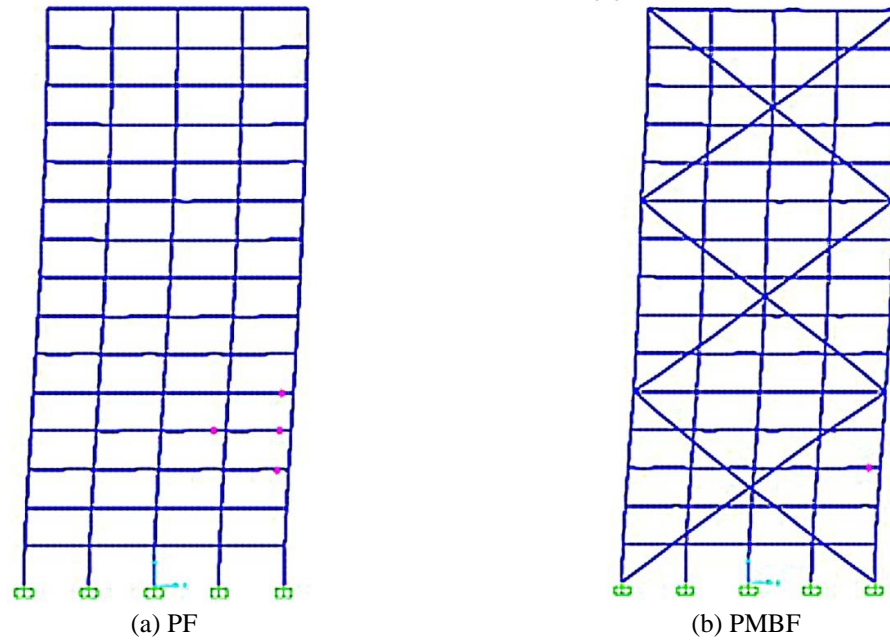


Fig. 13 Plastic hinge distribution when it begins to appear in beam under inverted triangular horizontal load

Plastic hinges begin to appear in the frame columns for PF at the load of 195.83 kN with the roof drift of 638.16 mm. For PMBF, plastic hinges begin to appear in the columns of the bottom

mega-frame at the load of 784.42 kN with the roof drift of 480.68 mm, as shown in Fig. 11.

PF reaches its ultimate bearing capacity at the load of 205.44 kN with the roof drift of 908.53 mm. PMBF reaches its ultimate bearing capacity at 885.90 kN with the roof drift of 563.16 mm, as shown in Fig. 12.

#### 4.3.2 Inverted triangular distribution

Plastic hinges begin to appear in the frame beams for PF at the load of 133.93 kN with the corresponding roof drift of 439.05 mm. For PMBF, plastic hinges start in the frame beams of the first mega-frame at the load of 522.11 kN with the roof drift of 411.20 mm, as shown in Fig. 13.

Plastic hinges begin to appear in the frame columns for PF at the load of 159.13 kN with the roof drift of 672.04 mm. For PMBF, plastic hinges start in the frame columns of the third mega-frame at the load of 585.69 kN with the roof drift of 468.47 mm, as shown in Fig. 14.

PF reaches its ultimate bearing capacity at the load of 170.21 kN with the roof drift of 968.20 mm. When the horizontal load is 791.11 kN with the roof drift is 686.06 mm, many plastic hinges are formed in PMBF. At the same time, plastic hinges begin to appear in the cables of the bottom mega-frame, and PMBF reaches its ultimate bearing capacity, as shown in Fig. 15.

It can be seen from the above analysis that no matter what lateral load pattern is, in PMBF the beams yield first and then the columns. Because of its high strength, the cables will not yield until the structure reaches its limit state. This is a desired failure mode from the point view of energy dissipation, for energy dissipation is considerable when frame beams or columns yielding but relatively low for pre-stressed cables. Moreover, from the point view of collapse resistance, delayed cable yielding is obviously beneficial to prevent the structure from transforming into a mechanism.

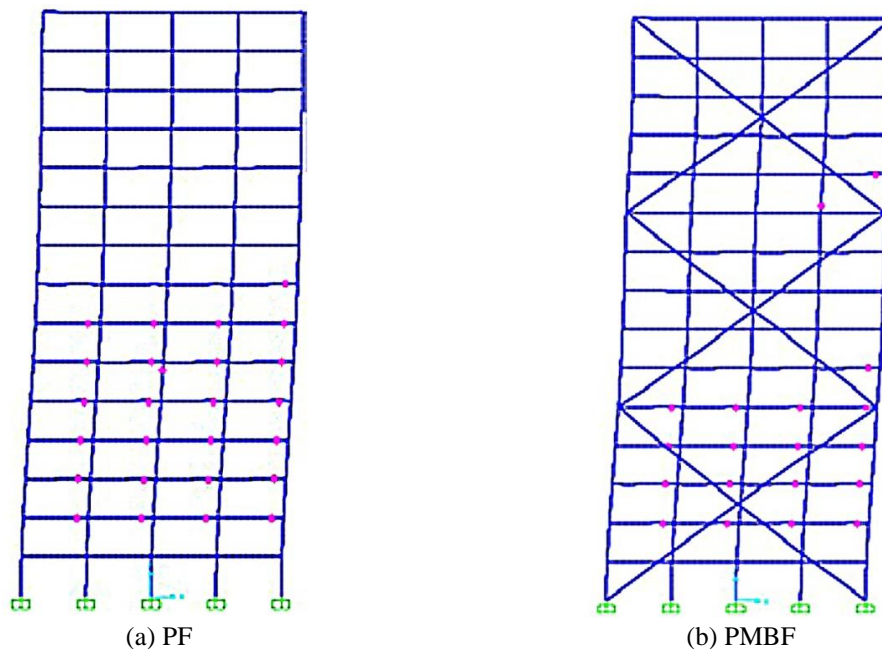


Fig. 14 Plastic hinge distribution when it begins to appear in column under inverted triangular horizontal load

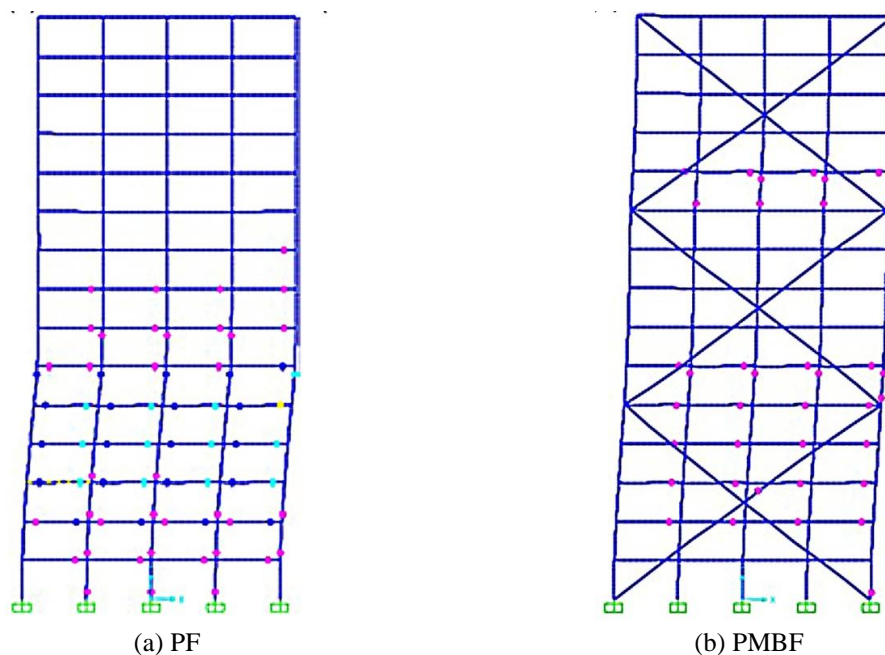


Fig. 15 Plastic hinge distribution when the ultimate bearing capacity state is reached under inverted triangular horizontal load

Table 4 Lateral stiffness of each destruction stage (unit: kN/mm)

Horizontal load mode	Structure type	Plastic hinges formed in beams	Plastic hinges formed in columns	Ultimate bearing capacity state
Uniform distribution	PF	0.41	0.31	0.23
	PMBF	1.70	1.63	1.57
Inverted triangular distribution	PF	0.31	0.24	0.18
	PMBF	1.27	1.25	1.15

According to the above data, the lateral stiffness in each destruction stage for the two structures can be obtained as shown in Table 4.

Under the three typical states, the lateral stiffness of PMBF is 4, 5, and 6.5 times that of PF. It can be seen that, for both PF and PMBF, the bearing capacity and lateral stiffness under the inverted triangular distribution are less than those under the uniform distribution. Therefore, the inverted triangular distribution is an unfavorable load distribution.

#### 4.4 Cable parameter analysis

To study the influence of the cable parameters on PMBF, based on the data in Table 2, the pretension and diameter of the pre-stressed cables were varied by 20%.

##### 4.4.1 Fluctuation in cable pretension by 20%

Figs. 16-17 respectively show the base shear-roof drift curves and lateral stiffness-roof drift

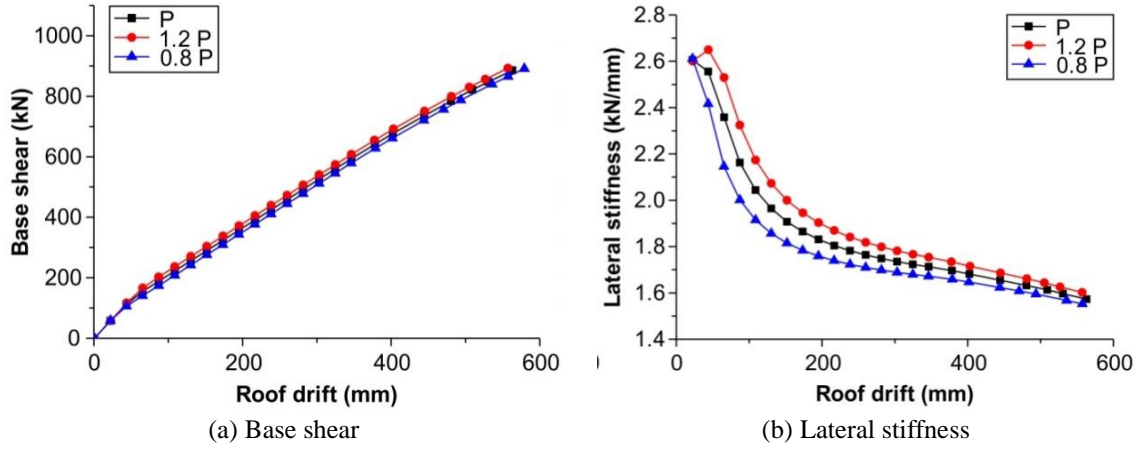


Fig. 16 Base shear and lateral stiffness curves under uniformly horizontal load

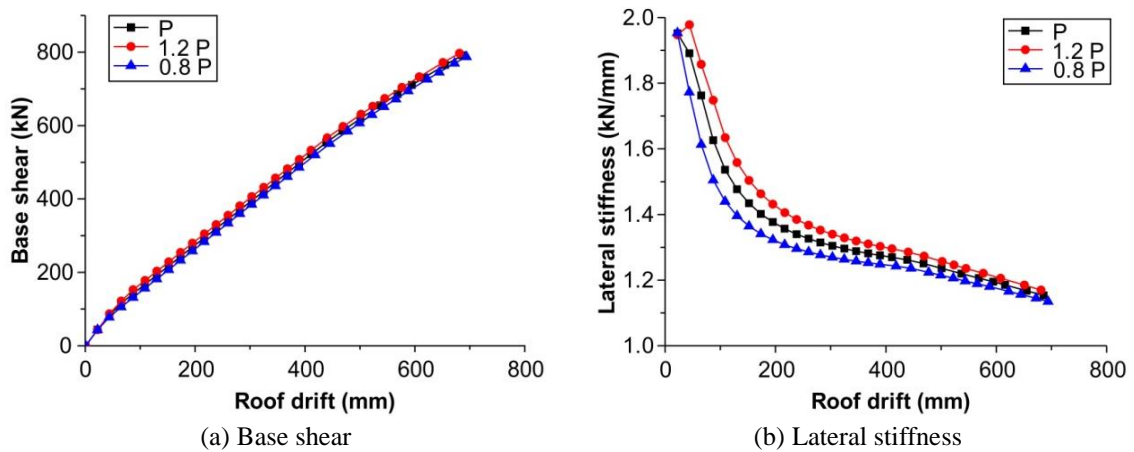


Fig. 17 Base shear and lateral stiffness curves under inverted triangular horizontal load

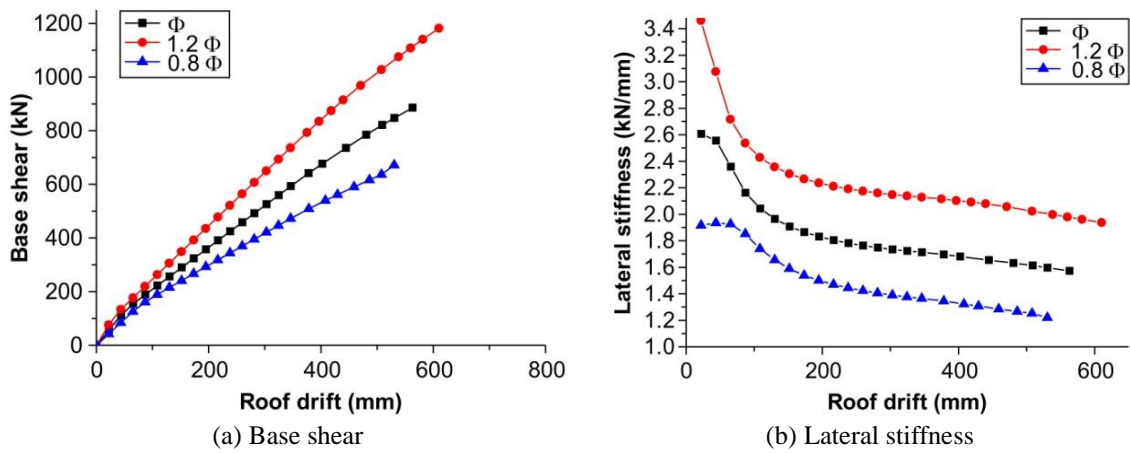


Fig. 18 Base shear and lateral stiffness curves under uniformly horizontal load

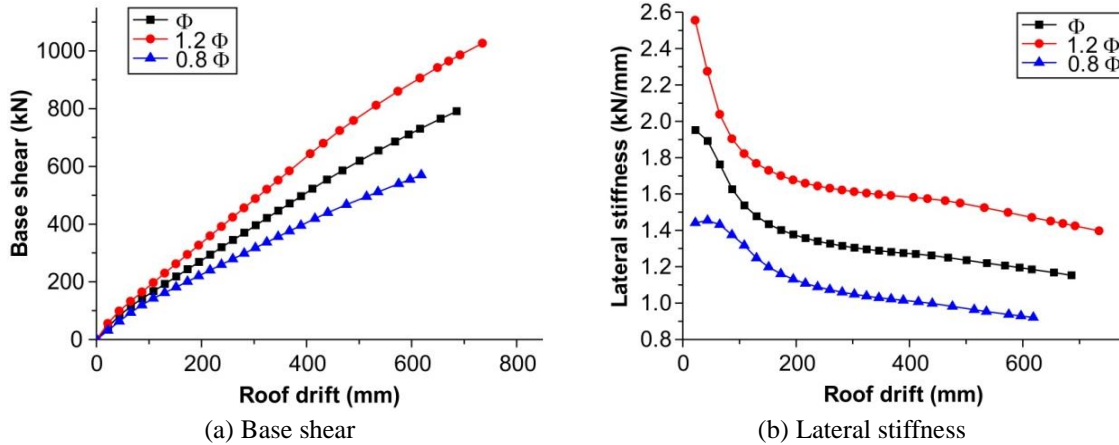


Fig. 19 Base shear and lateral stiffness curves under inverted triangular horizontal load

curves under three different cable pretensions where  $P$  is the cable pretension shown in Table 2. The fluctuation in the cable pretension has little effect on the ductility, bearing capacity, and lateral stiffness.

#### 4.4.2 Fluctuation in cable diameter by 20%

Figs. 18-19 respectively show the base shear-roof drift curves and lateral stiffness-roof drift curves under three different cable diameters where  $\Phi$  is the cable diameter shown in Table 2. The 20% fluctuation in the cable diameter of PMBF causes 20%-30% fluctuation in the ultimate bearing capacity and 15%-20% fluctuation in the structural lateral stiffness.

## 5. Conclusions

The following conclusions can be drawn from this study:

- Cable braces can effectively improve the lateral stiffness and bearing capacity of a steel frame and significantly reduce structural story drifts. However, it can also cause rapid degradation of the lateral stiffness and poor ductility.
- Under horizontal loads, in PMBF plastic hinge formation starts with the beam ends first, then propagates to the frame columns, and continues till the yielding of the pre-stressed cables.
- 20% fluctuation in the cable pretension has little effect on the structural bearing capacity and lateral stiffness. However, 20% fluctuation in the cable diameter has much greater impact.

## Acknowledgments

The research described in this paper was financially supported by Key Laboratory for Structure Engineering Science Research Program, Jiangsu Province, China (ZD1302) and Natural Science Fund for Colleges and Universities in Jiangsu Province, China (15KJB560004).

## References

- Asgarian, B. and Moradi, S. (2011), "Seismic response of steel braced frames with shape memory alloy braces", *J. Constr. Steel Res.*, **67**(1), 65-74.
- Asghari, A. and Gandomi, A.H. (2015), "Ductility reduction factor and collapse mechanism evaluation of a new steel knee braced frame", *Struct. Infrastr. Eng.*, **12**(2), 239-255.
- Chou, C.C., Chen, Y.C., Phama, D.H. and Truong, V.M. (2014), "Steel braced frames with dual-core SCBs and sandwiched BRBs: Mechanics, modeling and seismic demands", *Eng. Struct.*, **72**(1), 26-40.
- Esmaeili, H., Kheyroddin, A., Kafi, M.A. and Nikbakht H. (2013), "Comparison of nonlinear behavior of steel moment frames accompanied with RC shear walls or steel bracings", *Struct. Des. Tall Spec. Build.*, **22**(14), 1062-1074.
- FEMA 356 (2000), Prestandard and commentary for the seismic rehabilitation of buildings, Washington, USA.
- Gu, S., Tang, B.J. and Shao, J.H. (2011), "Estimation theory on cable's diameter in prestress mega brace and steel frame structure", *Appl. Mech. Mater.*, **94**, 310-315.
- Khandelwal, K., EI-Tawil, S. and Sadek, F. (2009), "Progressive collapse analysis of seismically designed steel braced frames", *J. Constr. Steel Res.*, **65**, 699-708.
- Kim, D.H., Lee, C.H., Ju, Y.K. and Kim, S.D. (2014), "Subassemblage test of buckling: Restrained braces with H-shaped steel core", *Struct. Des. Tall Spec. Build.*, **24**(1), 243-256.
- GB50017 (2003), Chinese code for design of steel structures, Beijing. (in Chinese)
- GB50011 (2010), Chinese code for seismic design of buildings, Beijing. (in Chinese)
- GB50009 (2012), Chinese load code for the design of building structures, Beijing. (in Chinese)
- Pandikkadavath, M.S. and Sahoo, D.R. (2015), *Advances in Structural Engineering*, Springer India, New Delhi, India.
- Tang, B.J. and Gu, S. (2010), "Displacement mode of pre-stress-mega-braced steel frames", *Build. Sci.*, **26**(9), 57-61. (in Chinese)
- Tang, B.J. and Gu, S. (2010), "Rule of initial prestress in prestress-mega-braced steel frame", *J. Shenyang Jianzhu Univ. (Nat. Sci.)*, **26**(3), 480-484. (in Chinese)